



Unsaturated polyester resin/aluminum tri-hydroxide added with short glass fiber for battery box

S. Kaleg^{a*} • Sudirja^a • A. C. Budiman^a • Amin^a • A. Muharam^a •
A. Hapid^a • K. Diharjo^b • D. Ariawan^b

^aResearch Center for Transportation Technology, National Research and Innovation Agency,
Bandung, Indonesia

^bDepartment of Mechanical Engineering, Faculty of Engineering,
Universitas Sebelas Maret, Surakarta, Indonesia

Received 01 19 2022; accepted 09 01 2022

Available 06 30 2023

Abstract: Composite polymer samples of unsaturated polyester (UP) resin combined with aluminum tri-hydroxide (ATH) and short glass fiber (G) mixture to increase flame retardancy and mechanical strength has been experimentally studied. The UP with ATH and G has a lower burning rate and better thermal stability than the neat UP, based on the burning test, DSC, and TGA measurements. For the mechanical properties, the UP/ATH/G2 sample showed an optimal composition compared to other filler compositions with a tensile strength of 41.5 MPa. This composition also produces an optimal bending strength of 68.9 MPa, higher than the neat UP. These results were confirmed by SEM observations, in which G particles exfoliate in the UP. The broken G particles on the fracture surface observation prove the good interlock bonding between UP and G. This evidence suggests that G increases the mechanical strength, making the composite suitable for battery box application.

Keywords: Flame retardancy, mechanical strength, unsaturated polyester, aluminum tri-hydroxide, short glass fiber

*Corresponding author.

E-mail address: suna024@brin.go.id (S. Kaleg).

Peer Review under the responsibility of Universidad Nacional Autónoma de México.

1. Introduction

Electrification in the transportation sector continues to increase along with the need for green technology. Several countries have made plans and calculations about the impact of electrification in the transportation sector (Brown et al., 2020; Holland et al., 2021; Liang et al., 2019; Mahady et al., 2020; Talebian et al., 2018). Regulations and incentives have been created so that the electrification targets can be quickly achieved. This encourages research and development of transportation technology, especially electric vehicles, to innovate soon (Amin et al., 2021; Budiman et al., 2021; Feng & Magee, 2020; Huda et al., 2020). However, there are still many challenges in electric vehicles and the development of their components. One of the development challenges is the battery pack. A typical battery pack consists of battery cells, a battery management system, connectors, fuses, a battery box, and wiring. A battery box is usually made from metal, such as mild steel (Yang et al., 2019), stainless steel (Masurkar et al., 2018), or aluminum alloy (Chen et al., 2017), which acts as a container and also as a flame barrier. The strength of the battery box structure is designed to support the weight of the battery cells and other components in it. The study of collision scenarios that impact the structure and damage to the battery box was carried out (Qiao, Yu, et al., 2021; Qiao, Zhanxi, et al., 2021; Ruan et al., 2021). Moreover, a battery box protects the external environment from the thermal runaway of the battery cells. The thermal runaway can occur due to over-current, over-voltage, and overcharge (Gao et al., 2022). At the same time, it also protects the battery cells from thermal exposure or flame from the external environment as mentioned in ISO 12405-3 standard (Darnikowski & Mieloszyk, 2021). When a vehicle accident causes a fire, the surrounding temperature may be higher than the internal temperature of the battery box. As a result, the battery cells become exposed so that the temperature increases. At extreme levels, this may lead to material decomposition in the battery cell (Kotak et al., 2021) and cause an internal short circuit or thermal runaway (Bisschop et al., 2019).

The additional battery capacity requires more material for the battery box, thus increasing the vehicle curb weight. Components that cause an increase in such curb weight are undesirable in designing a vehicle (Liu et al., 2020). Heavy vehicles require more energy than light vehicles (Nandhakumar et al., 2021). Specifically for electric vehicles, the high or low curb weight can influence the vehicle mileage on each battery charged (Kumar & Bharj, 2021). As an alternative, metal can be replaced with non-metallic materials but with the same function to achieve the goal of lightweight vehicles (Liu et al., 2018). The most popular non-metallic material is a polymer (Mutlu et al., 2021). Thermoplastic polymers have a high potential for use in the automotive

industry (Elmarakbi, 2014). The polymer can be combined with reinforcement to form a structure with a specific strength called polymer composites. In addition to being lightweight, some of the superior characteristics are the high strength, corrosion resistance, and fatigue resistance obtained from fiber-reinforced polymer (Xian et al., 2022). Glass fiber-reinforced polymer is an example of such a composite. Applying polymer composites to vehicle components can improve vehicle efficiency in the form of lower energy consumption (Wu et al., 2018). Reduction in the emission is the other advantage that can be obtained (Xian et al., 2022).

In this study, the polymer used as the base material for the battery box is unsaturated polyester (UP) resin. Polyester is widely used in composite products because it has good mechanical properties, resistant to weather changes, and is economical (Mouritz & Gibson, 2006). UP is a typical thermosetting polymer widely used in the composite industry in aerospace, automotive, transportation, and other fields because of its low viscosity and easy processing (Gao et al., 2020). Due to a viscous material, UP shows the potential that can be applied to various fabrication processes (Blanco et al., 2021), including hand lay-ups and spray lay-ups. Furthermore, another potential application of this material is to use it as a base material for thermal conductivity in the renewable energy fields (Bing et al., 2021). However, UP has an undesirable property when applied to a battery box, which is flammable. UP is a highly flammable material that produces toxic gas and releases lots of heat when decomposed (Chu et al., 2021). One of the solutions to this issue is adding flame retardant fillers, such as aluminum tri-hydroxide (ATH) (Zhang et al., 2021). ATH undergoes endothermic decomposition starting at 220°C and produces an enthalpy of water release of 1.17 kJ/g (Horrocks & Price, 2001). ATH decomposes to produce alumina (Al₂O₃) and water (H₂O). Alumina is a flame retardant that forms a barrier after ATH decomposition, while water dissolves combustible materials causing a decrease in fire reactivity (Visakh & Yoshihiko, 2015). The addition of ATH into UP can increase ignition time, reduce carbon monoxide gas yield, and decrease peak heat release rate, hence increasing the level of safety (Chai et al., 2019; Hapuarachchi & Peijs, 2009). UP with an ATH composition of 60wt% can produce flame retardancy according to UL-94 V0 (Colpankan et al., 2018). Even UP with nanosized ATH particles produce higher flame retardancy than micro-sized ones (Elbasuney, 2017). The negative impact that arises from ATH concentration in the UP is a decrease in the mechanical properties of the composite. When the ATH composition is more than 10wt%, the tensile strength of the UP composite is lower than the neat UP (Zhao et al., 2010). Likewise, the flexural strength also tends to decrease along with the increase in ATH (Kaleg et al., 2018). The increase of filler content causes a reduction of the ultimate tensile strength of the composites due to the lack of polymer

(Bleach et al., 2002). Even when added with reinforcement fiber, the combination of UP and ATH still decreases flexural strength (Kaleg et al., 2022). The mechanical properties degradation of the UP with ATH for battery boxes needs to be re-evaluated due to the vehicle will operate dynamically because of acceleration, deceleration, and road surface that produce vibrations in the structure. The mass of battery cells can provide static and dynamic loads on the battery box. These operating conditions cause the combination of UP and ATH may not be appropriate as a battery box material.

ATH can be combined with other fillers as a hybrid in the UP to reduce the degradation of mechanical properties. The combination with a reinforcement powder may improve mechanical properties and flame retardancy optimally (Bhaskar et al., 2020), even though this powder comes from synthetic or natural materials (Chandramohan & Kumar, 2017). Silicon carbide, aluminum oxide, Calcium carbonate, Boron carbide, Zinc oxide, and Graphite are some synthetic powders that can improve the mechanical properties of polymer composites (Praveenkumara et al., 2021). Rice husk, coconut shell filler, egg shells filler, fish bone and fish scale filler, peanut and groundnut shell powder, and wood sawdust are natural materials that have the advantages of abundant availability, biodegradable, inexpensive, low specific density, non-toxic, and environmentally friendly (Jagadeesh et al., 2020).

The solution proposed in this study is to combine ATH and short glass fiber (G). Filler G is a powder material usually used in industry to increase the strength of polymer composites. The G of up to 20% to the UP can increase the composite flexural strength by 56% and tensile strength by 15% more than neat ones (Mubeen et al., 2019). Hybrid fillers between porcelain powder and glass powder can increase the compressive strength and modulus of elasticity of the epoxy composites (Salih et al., 2018). A specific composition between UP, ATH, and G will produce an optimal balance of flame retardancy and mechanical strength. An experimental study was carried out to characterize several samples of UP composites with variations of ATH and G. This paper describes the experiments starting from the materials used, the composites characterization, and discussions regarding the results and observations.

2. Materials and methods

2.1. Materials

The polymer material in this study is unsaturated polyester (UP) mixed with aluminum tri-hydroxide (ATH) and short glass fiber (G) as the fillers. The UP used is an orthophthalic, thixotropic, pre-accelerated, and non-waxed resin manufactured by Justus Kimiaraya with the brand name Yukalac 157 BQTN-EX. The methyl ethyl ketone peroxide (MEKP) is a solution that triggers the cure reaction process of

the UP composites, supplied by Justus Kimiaraya with the brand name MEPOXE. Technical grade ATH was a flame retardant obtained from ROFA laboratory center with the product code of RLC2.0008.1000. This ATH filler has a material density of 2.42 g/mL and a purity of more than 95%. Filler G as the composite reinforcement is a silica-rich micro-sized fiber material obtained from Justus Kimiaraya with the product name of Glassron powder. Figure 1 shows the morphology and grain size of the ATH and G particles. ATH particles are predominantly oval with a length of about 18 to 24 μm and a width of about 12 to 15 μm . Irregular ATH particles were observed because of the absence of a sieving process for ATH preparation. G particles form and size are cylindrical rods with a diameter of about 12 μm and a length of about 100 to 500 μm .

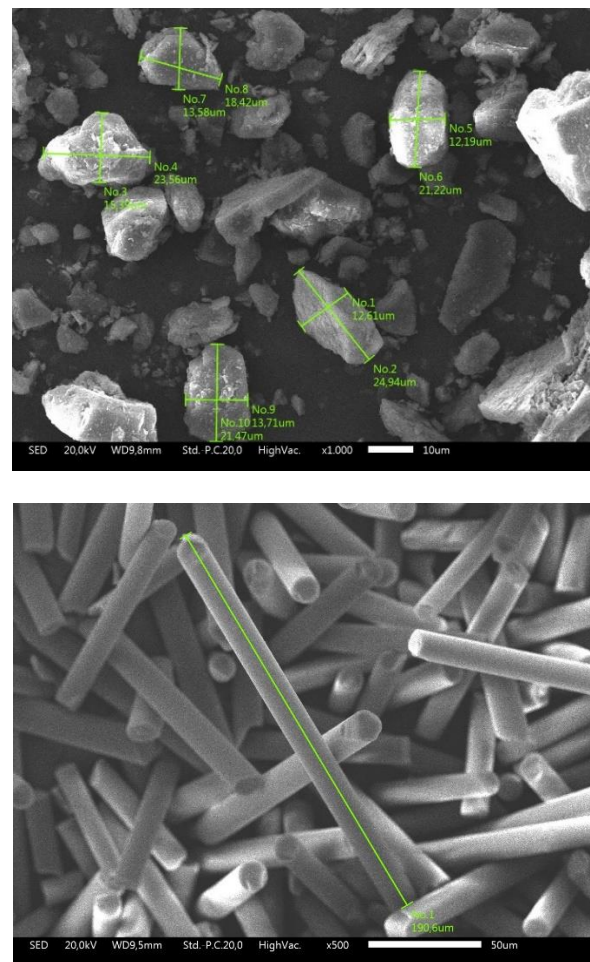


Figure 1. The morphology and particles size: (a) ATH and (b) G.

2.2. Samples preparation

Table 1 presents the weight percentage of neat UP and UP composite samples. The composite materials were mixed in a high-speed mechanical mixer to increase the dispersion of the filler into the resin. The UP and the fillers were stirred at 3,000

rpm for 5 minutes (Hapuarachchi & Peijs, 2009). The matrix (already mixed materials) was stored until the trapped bubbles during the mixing process were visually released. Next, MEKP as much as 1wt% of UP was added into the matrix and stirred slowly until evenly blended. The matrix was poured into an open mold to produce samples. The matrix was stored at room temperature for 24 hours for the slow curing process. Finally, the samples were released from the mold and then put into an oven with circulated air for a post-curing process for 60 minutes at 100 °C (Diharjo et al., 2013).

Table 1. Formulation of the UP composites.

Sample code	Composition (wt%)		
	UP	ATH	G
UP	100	0	0
UP/ATH	75	25	0
UP/ATH/G1	75	23	2
UP/ATH/G2	75	21	4
UP/ATH/G3	75	19	6
UP/ATH/G4	75	17	8

2.3. Characterization

The characterization of flame retardancy and mechanical properties is implemented in all the composite samples (following Table 1). Flame retardancy was measured through thermal properties, thermal stability analysis, and burning properties. Furthermore, the mechanical properties were measured through tensile strength, bending strength, and observation of the fracture surface morphology. Thermal properties were investigated by measuring the endothermic peak temperature of the samples. The endothermic temperature was measured using the differential scanning calorimetry (DSC) of NETZSCH DSC 214 Polyma. The DSC temperature range was from 30 to 180 °C at a heating rate of 4 °C/min. The thermal stability properties of samples were investigated using thermogravimetric analysis (TGA) utilizing NETZSCH TG 209 F1 Libra. The TGA temperature range was from 25 to 600 °C at a heating rate of 20 °C/min and under an N₂ atmosphere (the flow rate is 20 mL/min). The burning properties were examined according to the ASTM D 635 standard. The test data is in the form of the burning rate (V in mm/min) calculated from the burning time (t in min) and burning length (L in mm), which refers to a formula in (1).

$$V = \frac{60L}{t} \quad (1)$$

The strength of materials tests was applied to the samples to analyze the effect of adding ATH and G into UP. The tensile and bending strength were measured using a universal testing machine of the Tensilon UCT series. The crosshead speed of tensile and bending strength tests was 10 mm/min and 2

mm/min, respectively. The tensile and bending samples were characterized according to the ASTM D 638 and ASTM D 790 standards, respectively. The fracture surface of the samples was observed using scanning electron microscopy (SEM) of JEOL JSM-IT300.

3. Results and discussion

3.1. Thermal properties

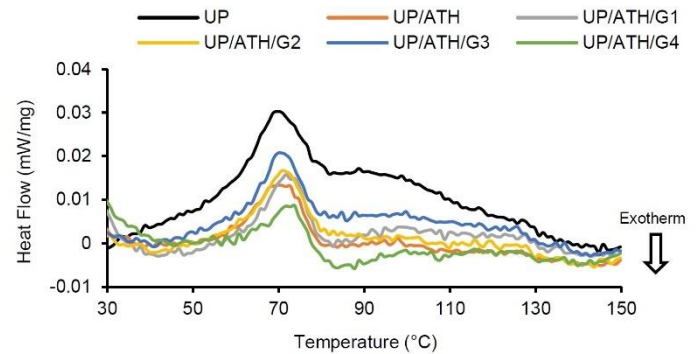


Figure 2. DSC thermograms of UP composites examined at a heating rate of 4 °C/min.

The DSC thermograms of the samples are depicted in Figure 2. The maximum endothermic temperature is shown from the peaks on the heat flow curve. The DSC results show that the maximum endothermic for each sample occurs at a temperature of around 70 °C by the nature of the thermoset material, which has a visible glass transition effect (Salasinska et al., 2020). The same results were also shown in a study on epoxy resins with flame retardant ATH (Budd & Cree, 2019). Table 2 shows that the samples with the addition of G had a higher maximum endotherm temperature than UP and UP/ATH. The UP/ATH/G4 shows the highest maximum endotherm temperature with an increase of 2.7 °C to the UP. The addition of G by 8wt% influences this result since the main compositions of filler G are Si, Ca, and Al. These elements are heat absorbents that work to reduce the rate of thermal distribution to an extended area. Silica (SiO₂) can slow down the polymer decomposition rate, but a significant effect appears at a temperature of 250 to 500 °C (Wang et al., 2013). The addition of alumina (Al₂O₃) content can increase the glass transition temperature due to increasing endothermic reactions (Chen et al., 2022). These results prove that filler G acts as a heat sink in the UP resin. Silica can significantly reduce the peak heat release rate of polymer materials (Czlonka et al., 2020). The UP/ATH shows a slight increase in maximum endotherm temperature of 0.8°C to the UP. The ATH also functions as a heat sink in the UP resin (Elbasuney, 2017; Hapuarachchi & Peijs, 2009). Another study showed that the

addition of ATH did not modify the melting point temperature of polymer composites (Chang et al., 2014). However, ATH can withstand composite degradation to higher temperatures than without metal hydroxides (Fredi et al., 2019). The heat sink effect is beneficial to the function of the battery box components. Certain shapes and materials can produce a more efficient thermal conductivity as a heat sink (Akula & Balaji, 2022). This heat sink effect causes heat exposure from outside the battery box retained before reaching the battery cell assembly. On the other hand, the fire hazard that may be caused by the thermal runaway of the battery cells can be restrained by the battery box material to provide sufficient evacuation time for people around the vehicle.

3.2. Thermal stability analysis

The degradation of weight due to temperature is discussed in three stages in the form of the temperature at 95% weight (T_{95}), the temperature at weight 50% (T_{50}), and the temperature at the maximum value of the derivative of weight (T_{max}). Furthermore, the final weight at a temperature of 600 °C (FW) and the maximum rate of weight degradation (DTG_{max}) strengthen the thermal stability discussion. Figure 3 shows the TGA thermogram for each sample and is clarified by the TGA and DTG data in Table 3. When T_{95} occurs, the inset in the TGA results shows that the samples added with ATH and G fillers have a higher temperature than the neat UP. The UP/ATH/G1 shows the highest temperature at a 95% weight of 258 °C.

Table 2. DSC data of the samples.

Sample	Maximum endotherm temperature (°C)
UP	70.1
UP/ATH	70.9
UP/ATH/G1	71.7
UP/ATH/G2	71.7
UP/ATH/G3	71.7
UP/ATH/G4	72.8

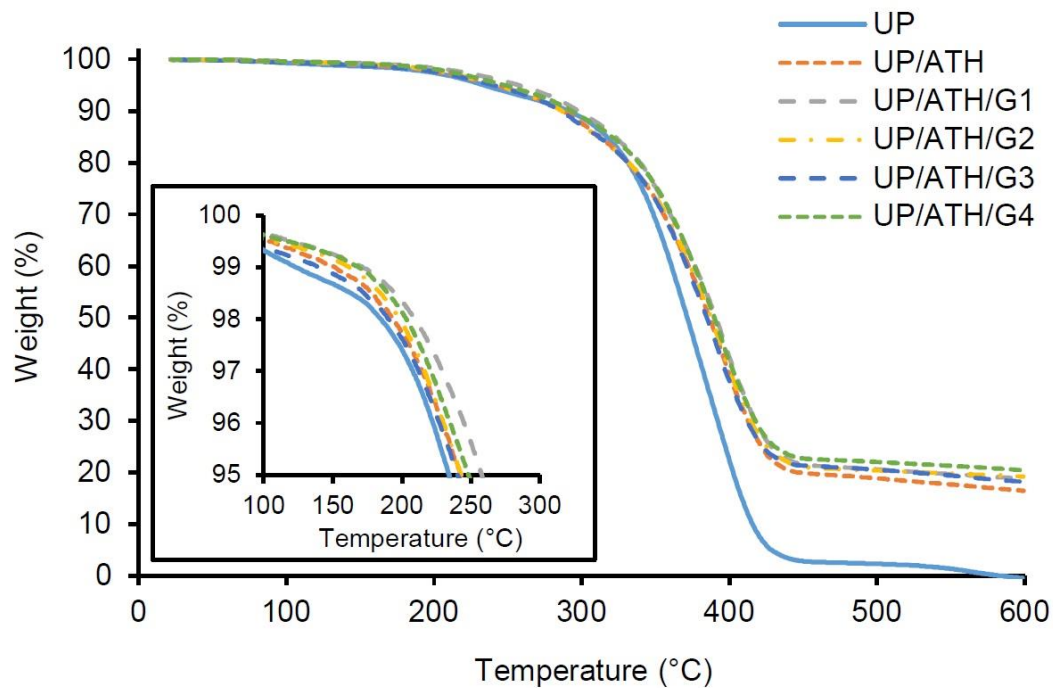


Figure 3. TGA thermograms of samples examined at a heating rate of 20 °C/min.

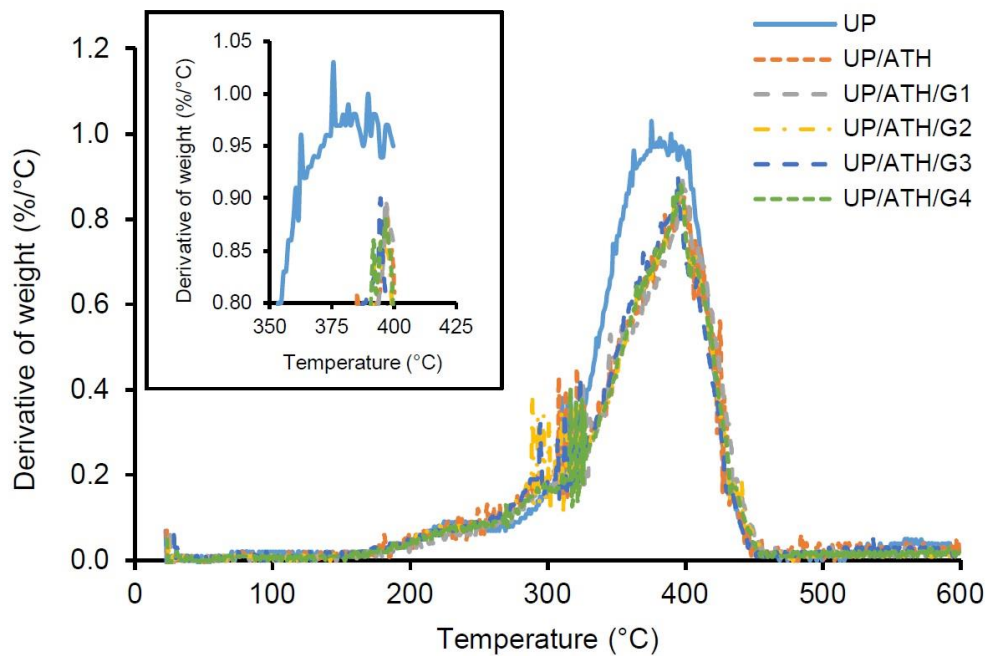


Figure 4. Derivative thermograms (DTG) of each sample.

Table 3. TGA and DTG data of samples.

Sample	T_{95}^1 (°C)	T_{50}^2 (°C)	T_{max}^3 (°C)	FW ⁴ (%)	DTG_{max}^5 (%/°C)
UP	234	372	377.8	0.0	1.03
UP/ATH	242	386	394.6	16.5	0.89
UP/ATH/G1	258	391	397.4	18.8	0.90
UP/ATH/G2	242	387	394.8	19.3	0.85
UP/ATH/G3	240	384	393.6	18.3	0.90
UP/ATH/G4	248	390	395.3	20.5	0.88

- 1) T_{95} is the temperature at 95% weight.
- 2) T_{50} is the temperature at 50% weight.
- 3) T_{max} is temperature derivative of weight.
- 4) FW is the final weight temperature of 600 °C.
- 5) DTG_{max} is the derivative of weight.

In T_{50} , the samples with the ATH and G fillers can maintain the weight better than neat UP. The UP/ATH/G1 has the highest temperature at 391 °C or about 5% higher than the neat UP. The maximum temperature value of the derivative of weight is used to analyze the temperature of the samples when they are at the highest weight degradation rate. The UP/ATH/G1 has the highest temperature in the highest weight degradation rate at 397.4 °C. The samples with ATH and G fillers leave about 16.5% to 20.5% residue at a temperature of 600 °C, which is in the form of char yield. ATH and G show better char-forming ability than neat UP (Tang et al., 2019). However, the samples with the addition of G showed more char yield than samples that only

used ATH. The ATH decomposition produces alumina (Al_2O_3) and water. Alumina has a lighter density than glass material (rich in Si). Char formed at high temperatures indicates an increase in the thermal stability of the polymer composite (Wang et al., 2003). The maximum rate of weight degradation is shown in Figure 4 and the value of DTG_{max} is in Table 3. In general, the addition of ATH and G fillers can reduce the rate of weight degradation due to a temperature of around 0.1%/°C. The samples with the addition of filler showed a slower rate of weight degradation compared to the neat material. The results prove that ATH and G can maintain the stability of UP by being degraded at higher temperatures (Suoware et al., 2019). The increase in UP stability is

caused by the barrier effect of the active filler when the material decomposes due to thermal (Tibiletti et al., 2011). Based on this thermal stability analysis, a battery box can be developed from UP by adding ATH and G fillers according to the composition of UP/ATH/G1. The advantage obtained is a box with better resistance to heat exposure.

3.3. Burning properties

According to Table 4, the samples with additional ATH and G fillers produced a lower burning rate than neat UP. The UP/ATH is the sample with the highest ATH composition resulting in the lowest burning rate of 6.9 mm/min, or 53% lower than neat UP. Adding ATH to the UP can reduce the value of the burning rate, which means an increase in flame retardancy. The 60wt% of ATH in the UP results in a composite that self-extinguished when burned (Kaleg et al., 2022). Several other studies showing a similar trend that increasing ATH concentrations can reduce the burning rate were found in polyvinyl alcohol (Ameer & Habbeeb, 2017) and bio-based polyurethane foam (Silva et al., 2021), while another one shows the flaming combustion is also self-extinguished (Halim et al., 2020; Marques et al., 2018). The mechanism of ATH during decomposition was endothermic dehydration by releasing water vapor and forming alumina formation (Hapuarachchi & Peijs, 2009). The formation of alumina in the polymer decomposition process makes air and fuel difficult to mix, which is a component of a fire.

Table 4. Burning rate data of the samples.

Sample	Burning rate (mm/min)	Standard deviation
UP	14.9	0.4
UP/ATH	6.9	0.2
UP/ATH/G1	8.4	0.4
UP/ATH/G2	8.5	0.3
UP/ATH/G3	8.6	0.3
UP/ATH/G4	9.2	0.2

Samples that added filler G showed an increase in the burning rate probably caused by the ATH reduction. However, samples with filler G still produced a lower burning rate than neat UP. Filler G consists of an oxide material with a predominance of silica (SiO₂). Silica will form a silica barrier when polymer decomposition occurs. As a similar mechanism to alumina, this formation hinders the mixing of air and fuel. The disadvantage of G over ATH is it does not have a hydroxyl

group that can dehydrate when exposed to fire. Therefore, the flame retardancy of ATH is better than that of G. Another drawback is the possible shape and size of the particles of G, which are relatively larger than ATH. The cylindrical shape, like a rod, may cause the imperfect formation of the barrier. However, all samples added with filler were proven more flame resistant than neat UP. A study of a balanced combination of silica and ATH resulted in a fire self-extinguished in the UP composite (Halim et al., 2020). Further evaluation is the mechanical strength to find the optimum value of flame retardancy and mechanical strength.

3.4. Tensile and bending strength

Figure 5 shows that neat UP produces the highest tensile strength of 43.4 MPa. The tensile strength of the samples with fillers reduces from 4.2% to 15%. The sample with G shows higher tensile strength than the sample with ATH only, which is the highest value generated by the sample UP/ATH/G2. The UP/ATH/G2 shows a composite with optimal composition than the other samples. The optimal composition is related to the porosity that influences the strength of the composites (Lanzl et al., 2020). Porosity causes the composite strength to increase and decrease again, with an optimal turning point composition of 50 vol%. Another study also shows the same result that more composition of G causes a decrease in the mechanical properties of a composite (Ku & Wong, 2012). Based on these results, a battery box can be made of UP composite with ATH and G, but attention to the decrease in tensile strength is still required.

Figure 6 shows that the bending strength of samples with ATH and G is higher than that of neat UP. The addition of filler causes an increase in bending strength from 3.9% to 65.3%. The UP/ATH/G2 produces the highest bending strength of 68.9 MPa. The addition of a filler with a rigid character increases the bending strength of the sample. The addition of ATH to a composite did not have a significant impact on the stiffness of the material (Petersen et al., 2015). However, suitable compositions of G can increase the stiffness of the composite (Bhaskar et al., 2020; Ku & Wong, 2012). The short fiber shape of the G material can increase the bending strength of the composite (Nawafleh & Celik, 2020). The concentration and combination of fillers in UP cause an increase in composite stiffness, which is indicated by an increase in bending strength. This is in good agreement with the previous study (Misri et al., 2015). Based on these bending strength results, UP with ATH and G fillers is more appropriate to be applied to battery box components with a bending load direction, for example, the battery base.

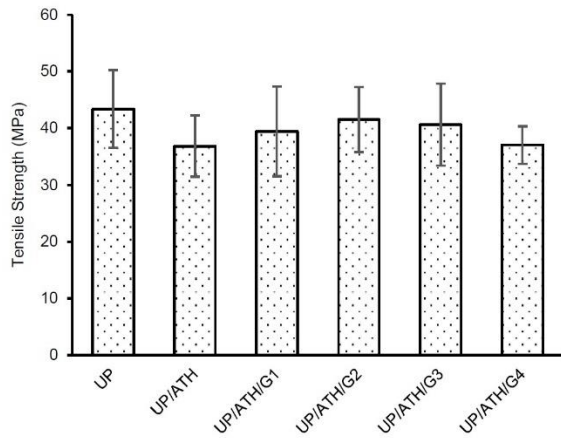


Figure 5. Tensile strength results.

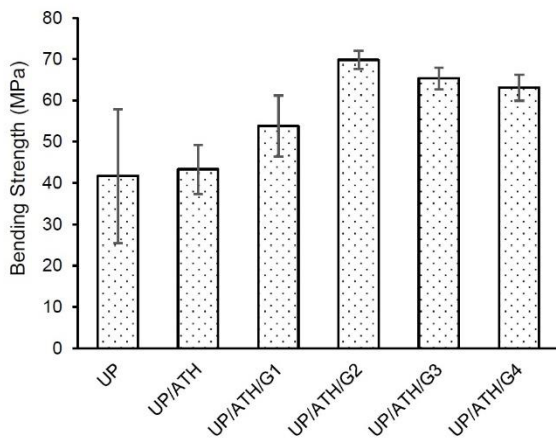


Figure 6. Bending strength results.

3.5. Morphology of the samples fracture surface

Observations on the morphology of the fracture surface of the mechanical test samples aim to determine the causes of the damage. Figure 7 is the fracture surface morphology of the UP/ATH/G2 sample. The observation result shows that the ATH and G particles were left behind and pulled out from the UP. The smooth cavity surface is evidence of weak interlock bonding between UP with ATH and UP with G. There is no visible structure observed between UP and fillers. The structure between UP and fillers can be made from a bonding agent which can react with the two composite components (Schuberth et al., 2016). ATH is a more rigid material than UP. The mechanical ability of a composite decreases in proportion to the addition of the ATH composition (Petersen et al., 2015). Figure 8 is a photograph of the ATH particles pulled out of the UP. The shape of the cavity follows the shape of the pulled-out ATH particles. The visible flakes are UP from a fractured sample. The G has a simpler shape than ATH, which is a cylindrical rod. Broken particles in Figure 9 prove good interlock bonding between UP and G. This filler increases the

bending strength of the UP composite, although some G particles were detached from the UP (Sodeifian et al., 2019). The UP/ATH/G2 shows the highest bending strength. Overall, UP with ATH and G remain higher bending strength than samples without G or neat UP. This can occur because the filler G spreads by exfoliation in the UP, which can improve the mechanical ability of a composite (Han et al., 2008).

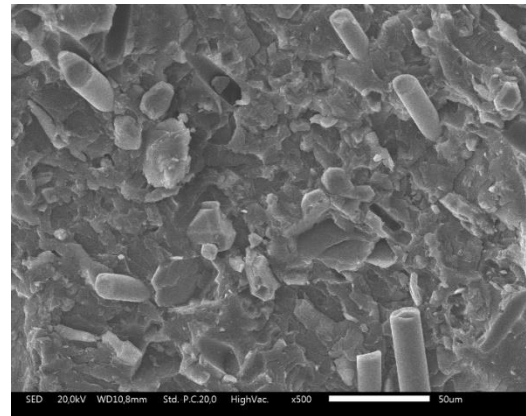


Figure 7. Fracture surface morphology of UP/ATH/G2.

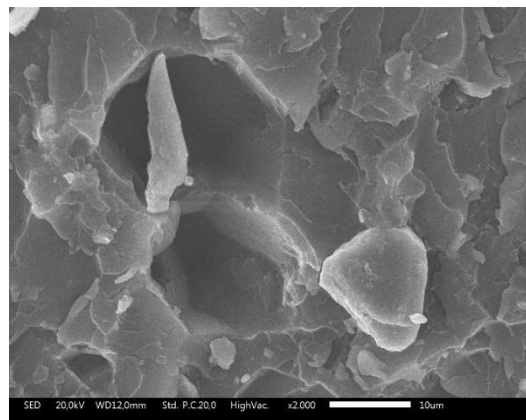


Figure 8. Pulled out ATH particle from UP.

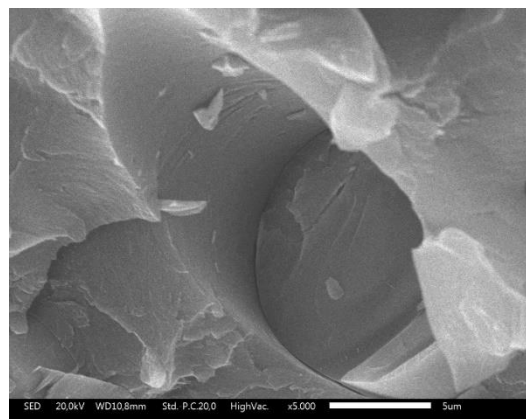


Figure 9. The fracture of G particle that is left in the UP.

Conclusions

An experimental study was carried out to characterize several samples of UP, ATH, and G composites. Certain ATH and G compositions (21% and 4%, respectively) in the UP/ATH/G2 produce optimal combustion resistance and mechanical strength. The DSC results for thermal properties show that the maximum endothermic of all samples occurs at a temperature of around 70 °C. Thermal stability analysis through TGA proves that ATH and G can maintain the stability of UP so that they are degraded at higher temperatures by reducing the rate of weight degradation due to a temperature of around 0.1%/°C. The burning properties also show that samples with additional ATH and G fillers have a lower burning rate value than neat UP. A battery box can be developed from UP by adding ATH and G fillers with better resistance to temperature exposure. For mechanical characterization, the tensile strength of the samples added with ATH and G fillers was lower than the neat UP. However, UP/ATH/G2 showed an optimal composition compared to other filler compositions with a tensile strength of 41.5 MPa. This sample also produces an optimal bending strength of 68.9 MPa, even higher than the neat UP. These results were confirmed by SEM observations, in which the filler G was exfoliated in the UP. Composite failure due to broken G particles proves good interlock bonding between UP and G so this filler contributes to the increase of the UP composite mechanical strength. The study shows an outline of material development for battery boxes from UP with ATH and G fillers. The UP/ATH/G2 shows the best compromise between mechanical strength and flame retardancy.

Conflict of interest

The authors do not have any type of conflict of interest to declare.

Acknowledgements

The authors acknowledge the facilities, scientific and technical support from Bandung Advanced Characterization Laboratories in National Research and Innovation Agency. S. Kaleg and Sudirja are the main contributors of this paper. All authors read and approved the final paper.

Funding

The authors received no specific funding for this work.

References

- Akula, R., & Balaji, C. (2022). Thermal management of 18650 Li-ion battery using novel fins-PCM-EG composite heat sinks. *Applied Energy*, 316, 119048. <https://doi.org/10.1016/j.apenergy.2022.119048>
- Ameer, Z. J. A., & Habbeeb, D. H. (2017). Effect of polyvinyl alcohol on burning rate for Flexible PVC with addition of magnesium hydroxide and Aluminum tri-hydroxide. *Journal of Babylon University/Engineering Sciences*, 25(2), 593-603.
- Amin, A., Budiman, A. C., Kaleg, S., Sudirja, S., & Hapid, A. (2021). Active battery balancing system for electric vehicles based on cell charger. *International Journal of Power Electronics and Drive Systems*, 12(1), 1729. <https://doi.org/10.11591/ijped.v12.i1.pp385-392>
- Bhaskar, K. B., Devaraju, A., & Paramasivam, A. (2020). Experimental investigation of glass powder reinforced polymer composite. *Materials Today: Proceedings*, 39, 484-487. <https://doi.org/10.1016/j.matpr.2020.08.211>
- Bing, N., Yang, J., Gao, H., Xie, H., & Yu, W. (2021). Unsaturated polyester resin supported form-stable phase change materials with enhanced thermal conductivity for solar energy storage and conversion. *Renewable Energy*, 173, 926-933. <https://doi.org/10.1016/j.renene.2021.04.033>
- Bisschop, R., Willstrand, O., Amon, F., & Rosengren, M. (2019). *Fire Safety of Lithium-Ion Batteries in Road Vehicles*. Retrieved from <https://urn.kb.se/resolve?urn=urn:nbn:se:ri:diva-38873>
- Blanco, M., Monteserín, C., Uranga, N., Gómez, E., Aranzabe, E., & García, J. I. (2021). Thermal and Photocatalytic Performance of Unsaturated Polyester Resins Modified with TiO₂ Nanoparticles as Panel Bodies for Vehicles. *Polymers*, 13(13), 2036. <https://doi.org/10.3390/polym13132036>
- Bleach, N. C., Nazhat, S. N., Tanner, K. E., Kellomäki, M., & Törmälä, P. (2002). Effect of filler content on mechanical and dynamic mechanical properties of particulate biphasic calcium phosphate - Polylactide composites. *Biomaterials*, 23(7), 1579-1585. [https://doi.org/10.1016/S0142-9612\(01\)00283-6](https://doi.org/10.1016/S0142-9612(01)00283-6)

- Brown, A. L., Fleming, K. L., & Safford, H. R. (2020). Prospects for a Highly Electric Road Transportation Sector in the USA. *Current Sustainable/Renewable Energy Reports*, 7(3), 84–93. <https://doi.org/10.1007/s40518-020-00155-3>
- Budd, R., & Cree, D. (2019). Effect of fire retardants on mechanical properties of a green bio-epoxy composite. *Journal of Applied Polymer Science*, 136(16), 1–10. <https://doi.org/10.1002/app.47398>
- Budiman, A. C., Kaleg, S., Hidayat, N. A., Silalahi, G. N., Gani, M. N., Muharam, A., & Hapid, A. (2021). Experimental study of two organic phase change materials in cylindrical containers for battery module thermal management: a comparative analysis. In *Journal of Physics: Conference Series* (Vol. 2047, No. 1, p. 012018). IOP Publishing. <https://doi.org/10.1088/1742-6596/2047/1/012018>
- Chai, G., Zhu, G., Gao, S., Zhou, J., Gao, Y., & Wang, Y. (2019). On improving flame retardant and smoke suppression efficiency of epoxy resin doped with aluminum tri-hydroxide. *Advanced Composites Letters*, 28, 1–12. <https://doi.org/10.1177/2633366X19894597>
- Chandramohan, D., & Kumar, A. J. P. (2017). Data in Brief Experimental data on the properties of natural fiber particle reinforced polymer composite material. *Data in Brief*, 13, 460–468. <https://doi.org/10.1016/j.dib.2017.06.020>
- Chang, M., Hwang, S., & Liu, S. (2014). Flame retardancy and thermal stability of ethylene-vinyl acetate copolymer nanocomposites with alumina trihydrate and montmorillonite. *Journal of Industrial and Engineering Chemistry*, 20(4), 1596–1601. <https://doi.org/10.1016/j.jiec.2013.08.004>
- Chen, Q. S., Zhao, H., Kong, L. X., & Chen, K. W. (2017). Research on battery box lightweight based on material replacement. In *2017 5th International Conference on Mechatronics, Materials, Chemistry and Computer Engineering (ICMMCCCE 2017)* (pp. 346-358). Atlantis Press. <https://doi.org/10.2991/icmmcce-17.2017.72>
- Chen, Y., Liu, S., Zhou, Y., Shang, P., Shan, Z., & Zhang, J. (2022). Effect of Al₂O₃ content on amorphous phase-separation and self-limited crystallization of phosphosilicate glasses. *Journal of Non-Crystalline Solids*, 584, 121505. <https://doi.org/10.1016/j.jnoncrysol.2022.121505>
- Chu, F., Xu, Z., Zhou, Y., Zhang, S., Mu, X., Wang, J., Hu, W., & Song, L. (2021). Hierarchical core-shell TiO₂@LDH@Ni(OH)₂ architecture with regularly-oriented nanocatalyst shells: Towards improving the mechanical performance, flame retardancy and toxic smoke suppression of unsaturated polyester resin. *Chemical Engineering Journal*, 405, 126650. <https://doi.org/10.1016/j.cej.2020.126650>
- Colpankan, O., Remzi, G., Alpay, G., Onur, T., Kandemir, K., Karaorman, A., & Albayrak, A. Z. (2018). Comparative Study on Flame Retardancy, Thermal, and Mechanical Properties of Glass Fiber Reinforced Polyester Composites with Ammonium Polyphosphate, Expandable Graphite, and Aluminum Tri-hydroxide. *Arabian Journal for Science and Engineering*, 43, 6211–6218. <https://doi.org/10.1007/s13369-018-3397-6>
- Członka, S., Strąkowska, A., Strzelec, K., Kairyte, A., & Kremensas, A. (2020). Melamine, silica, and ionic liquid as a novel flame retardant for rigid polyurethane foams with enhanced flame retardancy and mechanical properties. *Polymer Testing*, 87, 106511. <https://doi.org/10.1016/j.polymertesting.2020.106511>
- Darnikowski, D., & Mieloszyk, M. (2021). Investigation into the lithium-ion battery fire resistance testing procedure for commercial use. *Batteries*, 7(3), 1–16. <https://doi.org/10.3390/batteries7030044>
- Diharjo, K., Priyanto, K., Purwanto, A., Suharty, N. S., Jihad, B. H., Nasiri, S. J. A., & Widiyanto, D. (2013, November). Study of flexural strength on hybrid composite of glass/carbon-bisphenol for developing car body of electrical vehicle. In *2013 Joint International Conference on Rural Information & Communication Technology and Electric-Vehicle Technology (rICT & ICeV-T)* (pp. 1-4). IEEE. <https://doi.org/10.1109/rICT-ICeVT.2013.6741522>

- Elbasuney, S. (2017). Novel multi-component flame retardant system based on nanoscopic aluminium-trihydroxide (ATH). *Powder Technology*, 305, 538–545.
<https://doi.org/10.1016/j.powtec.2016.10.038>
- Elmarakbi, A. (2014). *Advanced Composite Materials for Automotive Applications: Structural Integrity and Crashworthiness*. John Wiley & Sons, Ltd.
- Feng, S., & Magee, C. L. (2020). Technological development of key domains in electric vehicles: Improvement rates, technology trajectories and key assignees. *Applied Energy*, 260, 114264.
<https://doi.org/10.1016/j.apenergy.2019.114264>
- Fredi, G., Dorigato, A., Fambri, L., Lopez-Cuesta, J.-M., & Pegoretti, A. (2019). Synergistic effects of metal hydroxides and fumed nanosilica as fire retardants for polyethylene. *Flame Retardancy and Thermal Stability of Materials*, 2, 30–48.
<https://doi.org/10.1515/flret-2019-0004>
- Gao, A., Dong, W., Xu, X., & Fan, L. (2022). Study on thermal runaway behavior of lithium ion battery under overcharge using numerical detecting method. In *Journal of Physics: Conference Series* (Vol. 2195, No. 1, p. 012017). IOP Publishing.
<https://doi.org/10.1088/1742-6596/2195/1/012017>
- Gao, W., Yu, Y., Chen, T., Zhang, Q., Chen, Z., Chen, Z., & Jiang, J. (2020). Enhanced flame retardancy of unsaturated polyester resin composites containing ammonium polyphosphate and metal oxides. *Journal of Applied Polymer Science*, 137(38), 49148.
<https://doi.org/10.1002/app.49148>
- Halim, Z. A. A., Yajid, M. A. M., Nurhadi, F. A., Ahmad, N., & Hamdan, H. (2020). Effect of silica aerogel – Aluminium trihydroxide hybrid filler on the physio-mechanical and thermal decomposition behaviour of unsaturated polyester resin composite. *Polymer Degradation and Stability*, 182, 109377.
<https://doi.org/10.1016/j.polyimdegradstab.2020.109377>
- Han, G., Lei, Y., Wu, Q., Kojima, Y., & Suzuki, S. (2008). Bamboo-fiber filled high density polyethylene composites: Effect of coupling treatment and nanoclay. *Journal of Polymers and the Environment*, 16(2), 123–130.
<https://doi.org/10.1007/s10924-008-0094-7>
- Hapuarachchi, T. D., & Peijs, T. (2009). Aluminium trihydroxide in combination with ammonium polyphosphate as flame retardants for unsaturated. *Express Polymer Letters*, 3(11), 743–751.
<https://doi.org/10.3144/expresspolymlett.2009.92>
- Holland, S. P., Mansur, E. T., Muller, N. Z., & Yates, A. J. (2021). The environmental benefits of transportation electrification: Urban buses. *Energy Policy*, 148, 111921.
<https://doi.org/10.1016/j.enpol.2020.111921>
- Horrocks, A. R., Price, D., & Price, D. (Eds.). (2001). *Fire retardant materials*. woodhead Publishing.
- Huda, N., Kaleg, S., Hapid, A., Kurnia, M. R., & Budiman, A. C. (2020). The influence of the regenerative braking on the overall energy consumption of a converted electric vehicle. *SN Applied Sciences*, 2(4), 1–8.
<https://doi.org/10.1007/s42452-020-2390-3>
- Jagadeesh, P., Puttegowda, M., Thyavihalli Girijappa, Y. G., Rangappa, S. M., & Siengchin, S. (2022). Effect of natural filler materials on fiber reinforced hybrid polymer composites: An Overview. *Journal of Natural Fibers*, 19(11), 4132-4147.
<https://doi.org/10.1080/15440478.2020.1854145>
- Kaleg, S., Budiman, A. C., Hapid, A., Muharam, A., Ariawan, D., & Diharjo, K. (2022). Evaluations of Aluminum Tri-Hydroxide and Pristine Montmorillonite in Glass Fiber Reinforced Polymer for Vehicle Components. *International Journal of Automotive and Mechanical Engineering (IJAME)*, 19(1), 9379–9390.
<https://doi.org/10.15282/ijame.19.1.2022.02.0721>
- Kaleg, S., Ariawan, D., & Diharjo, K. (2018). The flexural strength of glass fiber reinforced polyester filled with aluminum trihydroxide and montmorillonite. *Key Engineering Materials*, 772, 28–32.
<https://doi.org/10.4028/www.scientific.net/KEM.772.28>
- Kotak, B., Kotak, Y., Brade, K., Kubjatko, T., & Schweiger, H. G. (2021). Battery crush test procedures in standards and regulation: Need for augmentation and harmonisation. *Batteries*, 7(3), 63.
<https://doi.org/10.3390/batteries7030063>
- Ku, H., & Wong, P. (2012). Contrast on Tensile and Flexural Properties of Glass Powder Reinforced Epoxy Composites: Pilot Study. *Journal of Applied Polymer Science*, 123, 152–161.
<https://doi.org/10.1002/app.34469>

- Kumar, S., & Bharj, R. S. (2021). Experimental analysis of a light weight refrigerated electric vehicle in the summer and winter season. In *AIP Conference Proceedings* (Vol. 2317, No. 1, p. 030006). AIP Publishing LLC.
<https://doi.org/10.1063/5.0036461>
- Lanzl, L., Wudy, K., & Drummer, D. (2020). The effect of short glass fibers on the process behavior of polyamide 12 during selective laser beam melting. *Polymer Testing*, 83(October 2019), 106313.
<https://doi.org/10.1016/j.polymertesting.2019.106313>
- Liang, X., Zhang, S., Wu, Y., Xing, J., He, X., Zhang, K. M., Wang, S., & Hao, J. (2019). Air quality and health benefits from fleet electrification in China. *Nature Sustainability*, 2(10), 962–971.
<https://doi.org/10.1038/s41893-019-0398-8>
- Liu, Zhao, Zhu, C., Zhu, P., & Chen, W. (2018). Reliability-based design optimization of composite battery box based on modified particle swarm optimization algorithm. *Composite Structures*, 204, 239–255.
<https://doi.org/10.1016/j.compstruct.2018.07.053>
- Liu, Zongwei, Zhang, H., Hao, H., & Zhao, F. (2020). Comparative study of corporate average fuel consumption regulations based on curb weight and footprint benchmarks. *Clean Technologies and Environmental Policy*, 22, 1311–1323.
<https://doi.org/10.1007/s10098-020-01872-5>
- Mahady, J. A., Octaviano, C., Araiza Bolaños, O. S., López, E. R., Kammen, D. M., & Castellanos, S. (2020). Mapping Opportunities for Transportation Electrification to Address Social Marginalization and Air Pollution Challenges in Greater Mexico City. *Environmental Science and Technology*, 54(4), 2103–2111.
<https://doi.org/10.1021/acs.est.9b06148>
- Marques, D. V., Barcelos, R. L., Silva, H. R. T., Egert, P., Parma, G. O. C., Giroto, E., Consoni, D., Benavides, R., Silva, L., & Magnago, R. F. (2018). Recycled polyethylene terephthalate-based boards for thermal-acoustic insulation. *Journal of Cleaner Production*, 189, 251–262.
<https://doi.org/10.1016/j.jclepro.2018.04.069>
- Masurkar, N., Babu, G., Porchelvan, S., & Reddy Arava, L. M. (2018). Millimeter-scale lithium ion battery packaging for high-temperature sensing applications. *Journal of Power Sources*, 399, 179–185.
<https://doi.org/10.1016/j.jpowsour.2018.07.077>
- Misri, S., Sapuan, S. M., Leman, Z., & Ishak, M. R. (2015). Torsional behaviour of filament wound kenaf yarn fibre reinforced unsaturated polyester composite hollow shafts. *Materials & Design (1980-2015)*, 65, 953–960.
<https://doi.org/10.1016/j.matdes.2014.09.073>
- Mouritz, A. P., & Gibson, A. G. (2006). *Fire properties of polymer composite materials*. Springer Science & Business Media.
- Mubeen, M. A., Karunakar, C., & Sripathy, S. (2019). Preparation and testing of glass powder reinforced polyester resin lamina. *Materials Today: Proceedings*, 23, 608–612.
<https://doi.org/10.1016/j.matpr.2019.05.419>
- Mutlu, T., Yegin, S. K., Sen, G., & Dirikolu, M. H. (2021). 54.58 Design and implementation of a glass fiber reinforced hybrid polymer matrix composite washing machine drum support replacing cast aluminum alloy. *Composites Theory and Practice*, 21, 1-2.
- Nandhakumar, S., Seenivasan, S., Saalih, A. M., & Saifudheen, M. (2021). Weight optimization and structural analysis of an electric bus chassis frame. *Materials Today: Proceedings*, volume 37, part 2, 1824–1827.
<https://doi.org/10.1016/j.matpr.2020.07.404>
- Nawafleh, N., & Celik, E. (2020). Additive manufacturing of short fiber reinforced thermoset composites with unprecedented mechanical performance. *Additive Manufacturing*, 33, 101109.
<https://doi.org/10.1016/j.addma.2020.101109>
- Petersen, M. R., Chen, A., Roll, M., Jung, S. J., & Yossef, M. (2015). Mechanical properties of fire-retardant glass fiber-reinforced polymer materials with alumina tri-hydrate filler. *Composites Part B: Engineering*, 78, 109–121.
<https://doi.org/10.1016/j.compositesb.2015.03.071>
- Praveenkumara, J., Madhu, P., Gowda, T. G. Y., Sanjay, M. R., & Siengchin, S. (2021). A comprehensive review on the effect of synthetic filler materials on fiber-reinforced hybrid polymer composites. *The Journal of The Textile Institute*, 113(7), 1231–1239.
<https://doi.org/10.1080/00405000.2021.1920151>
- Qiao, W., Yu, L., Zhang, Z., & Pan, T. (2021). Study on the Battery Safety in Frontal Collision of Electric Vehicle. In *Journal of Physics: Conference Series* (Vol. 2137, No. 1, p. 012008). IOP Publishing.
<https://doi.org/10.1088/1742-6596/2137/1/012008>

- Qiao, W., Zhang, Z., Lu, D., & Yu, L. (2021). Study on Side Collision of Battery Boxes Based on HyperWorks. In *Journal of Physics: Conference Series* (Vol. 2137, No. 1, p. 012012). IOP Publishing.
<https://doi.org/10.1088/1742-6596/2137/1/012012>
- Ruan, G., Yu, C., Hu, X., Hua, J. (2021). Simulation and optimization of a new energy vehicle power battery pack structure. *Journal of Theoretical and Applied Mechanics*, 59(4), 565-578.
<https://doi.org/10.15632/jtam-pl/141503>
- Salasinska, K., Celinski, M., Barczewski, M., Leszczynski, M. K., Borucka, M., & Kozikowski, P. (2020). Fire behavior of flame retarded unsaturated polyester resin with high nitrogen content additives. *Polymer Testing*, 84, 106379.
<https://doi.org/10.1016/j.polymertesting.2020.106379>
- Salih, Y. A., Yass, M. F., Ahmed, A. S., & Abdulla, A. I. (2018). Effect of Adding Porcelain and Glass Powder Mixture on Epoxy Properties Effect of Adding Porcelain and Glass Powder Mixture on Epoxy Properties. *International Journal of Engineering & Technology*, 7(4.37), 39-42.
<https://doi.org/10.14419/ijet.v7i4.37.23612>
- Silva, E. H. P., Souza, G. S. C., Janes, D. B., Waldow, G., Sales, F. C. P., Guedes, R. M., Tita, V., & Costa, R. R. C. (2021). Flexural and flammability evaluation of a new bio-based polyurethane foam with alumina trihydrate. *Proceedings of the Institution of Mechanical Engineers, Part L: Journal of Materials: Design and Applications*, 235(5), 1160-1171.
<https://doi.org/10.1177/1464420720986591>
- Schuberth, A., Göring, M., Lindner, T., Töberling, G., Puschmann, M., Riedel, F., Scharf, I., Schreiter, K., Spange, S., & Lampke, T. (2016). Effect of new adhesion promoter and mechanical interlocking on bonding strength in metal-polymer composites. *IOP Conference Series: Materials Science and Engineering*, 118, 1-6.
<https://doi.org/10.1088/1757-899X/118/1/012041>
- Sodeifian, G., Ghaseminejad, S., & Yousefi, A. A. (2019). Preparation of polypropylene/short glass fiber composite as Fused Deposition Modeling (FDM) filament. *Results in Physics*, 12, 205-222.
<https://doi.org/10.1016/j.rinp.2018.11.065>
- Suoware, T. O., Edelugo, S. O., Ugwu, B. N., Amula, E., & Digitemie, I. E. (2019). Development of flame retarded composite fibreboard for building applications using oil palm residue. *Materiales de Construcción*, 69(335), e197-e197.
<https://doi.org/10.3989/mc.2019.10418>
- Talebian, H., Herrera, O. E., Tran, M., & Mérida, W. (2018). Electrification of road freight transport: Policy implications in British Columbia. *Energy Policy*, 115, 109-118.
<https://doi.org/10.1016/j.enpol.2018.01.004>
- Tang, W., Cao, Y., Qian, L., Chen, Y., Qui, Y., Xu, B., & Xin, F. (2019). Synergistic Charring Flame-Retardant Behavior of Polyimide and Melamine Polyphosphate in Glass Fiber-Reinforced Polyamide 66. *Polymers*, 11, 1851.
<https://doi.org/10.3390/polym11111851>
- Tibiletti, L., Longuet, C., Ferry, L., Coutelen, P., Mas, A., Robin, J., & Lopez-cuesta, J. (2011). Thermal degradation and fire behaviour of unsaturated polyesters filled with metallic oxides. *Polymer Degradation and Stability*, 96(1), 67-75.
<https://doi.org/10.1016/j.polyimdegradstab.2010.10.015>
- Visakh, P. M., & Yoshihiko, A. (2015). *Flame retardants: Polymer blends, composites and nanocomposites*. Springer.
<https://doi.org/10.1007/978-3-319-03467-6>
- Wang, L., Sánchez-Soto, M., & MasPOCH, M. L. (2013). Polymer/clay aerogel composites with flame retardant agents: Mechanical, thermal and fire behavior. *Materials and Design*, 52, 609-614.
<https://doi.org/10.1016/j.matdes.2013.05.096>
- Wang, S., Hu, Y., Wang, Z., Yong, T., Chen, Z., & Fan, W. (2003). Synthesis and characterization of polycarbonate / ABS / montmorillonite nanocomposites. *Polymer Degradation and Stability*, 80(1), 157-161.
[https://doi.org/10.1016/S0141-3910\(02\)00397-X](https://doi.org/10.1016/S0141-3910(02)00397-X)
- Wu, Y., Xia, C., Cai, L., Garcia, A. C., & Shi, S. Q. (2018). Development of natural fiber-reinforced composite with comparable mechanical properties and reduced energy consumption and environmental impacts for replacing automotive glass-fiber sheet molding compound. *Journal of Cleaner Production*, 184, 92-100.
<https://doi.org/10.1016/j.jclepro.2018.02.257>
- Xian, G., Guo, R., & Li, C. (2022). Combined effects of sustained bending loading, water immersion and fiber hybrid mode on the mechanical properties of carbon/glass fiber reinforced polymer composite. *Composite Structures*, 281, 115060.
<https://doi.org/10.1016/j.compstruct.2021.115060>
- Yang, N., Fang, R., Li, H., & Xie, H. (2019). Dynamic and static analysis of the battery box structure of an electric vehicle. *IOP Conference Series: Materials Science and Engineering*, 688(3), 0-6.
<https://doi.org/10.1088/1757-899X/688/3/033082>

Zhang, M., Ye, W., & Liao, Z. (2021). Preparation, Characterization and Properties of Flame Retardant Unsaturated Polyester Resin Based on r-PET. *Journal of Polymers and the Environment*.

<https://doi.org/10.1007/s10924-021-02325-w>

Zhao, Q., Jia, Z., Li, X., & Ye, Z. (2010). Effect of Al (OH)₃ Particle Fraction on Mechanical Properties of Particle-Reinforced Composites Using Unsaturated Polyester as Matrix. *Fail. Anal. and Preven.*, 10, 515–519.

<https://doi.org/10.1007/s11668-010-9379-y>